Acta Neuropathol
DOI 10.1007/s00401-011-0924-x

ORIGINAL PAPER

MicroRNA-182 promotes leptomeningeal spread of non-sonic hedgehog-medulloblastoma

Alfa H. C. Bai · Till Milde · Marc Remke · Claudio G. Rolli · Thomas Hielscher · Yoon-Jae Cho · Marcel Kool · Paul A. Northcott · Manfred Jugold · Alexandr V. Bazhin · Stefan B. Eichmüller · Andreas E. Kulozik · Armin Pscherer · Axel Benner · Michael D. Taylor · Scott L. Pomeroy · Ralf Kemkemer · Olaf Witt · Andrey Korshunov · Peter Lichter · Stefan M. Pfister

Received: 25 August 2011 / Accepted: 22 November 2011

Abstract The contribution of microRNAs to the initiation, progression, and metastasis of medulloblastoma (MB) remains poorly understood. Metastatic dissemination at diagnosis is present in about 30% of MB patients, and is associated with a dismal prognosis. Using microRNA expression profiling, we demonstrate that the retinal miR-183–96–182 cluster on chromosome 7q32 is highly overexpressed in non-sonic hedgehog MBs (non-SHH-MBs). Expression of miR-182 and miR-183 is associated with cerebellar midline localization, and miR-182 is significantly overexpressed in metastatic MB as compared to non-metastatic tumors. Overexpression of miR-182 in non-SHH-MB increases and knockdown of miR-182 decreases cell migration in vitro. Xenografts overexpressing miR-182 invaded adjacent normal tissue and spread to the leptomeninges, phenotypically reminiscent of clinically highly

Electronic supplementary material The online version of this article (doi:10.1007/s00401-011-0924-x) contains supplementary material, which is available to authorized users.

A. H. C. Bai · M. Remke · M. Kool · A. Pscherer · P. Lichter · S. M. Pfister (✉)
Division of Molecular Genetics (B060),
German Cancer Research Center (DKFZ),
Im Neuenheimer Feld 280, 69120 Heidelberg, Germany
e-mail: s.pfister@dkfz.de

T. Milde · O. Witt
Clinical Cooperation Unit Pediatric Oncology (G340),
German Cancer Research Center (DKFZ), Heidelberg, Germany

T. Milde · M. Remke · A. E. Kulozik · O. Witt · S. M. Pfister
Department of Pediatric Oncology, Hematology and Immunology, University of Heidelberg, Heidelberg, Germany

C. G. Rolli · R. Kemkemer
Department of New Materials and Biosystems, Max Planck Institute for Intelligent Systems, Stuttgart, Germany

C. G. Rolli
Department of Biophysical Chemistry, Institute for Physical Chemistry, University of Heidelberg, Heidelberg, Germany

T. Hielscher · A. Benner
Division of Biostatistics (C060), German Cancer Research Center (DKFZ), Heidelberg, Germany

Y.-J. Cho
Department of Neurology and Neurological Sciences, Stanford University School of Medicine, Stanford, USA

P. A. Northcott · M. D. Taylor
Division of Neurosurgery, Arthur and Sonia Labatt Brain Tumor Research Centre, Hospital for Sick Children, University of Toronto, Toronto, Canada

M. Jugold
Division of Medical Physics in Radiology, German Cancer Research Center (DKFZ), Heidelberg, Germany

A. V. Bazhin
Department of Surgery, University of Heidelberg, Heidelberg, Germany

S. B. Eichmüller
Division Translational Immunology (D015), German Cancer Research Center (DKFZ), Heidelberg, Germany

S. L. Pomeroy
Department of Neurology, Children's Hospital Boston, Boston, USA

A. Korshunov
Department of Neuropathology, University of Heidelberg, Heidelberg, Germany

A. Korshunov
Clinical Cooperation Unit Neuropathology,
German Cancer Research Center, Heidelberg, Germany

Published online: 02 December 2011

aggressive large cell anaplastic MB. Hence, our study provides strong in vitro and in vivo evidence that miR-182 contributes to leptomeningeal metastatic dissemination in non-SHH-MB. We therefore reason that targeted inhibition of miR-182 may prevent leptomeningeal spread in patients with non-SHH-MB.

Keywords hsa-miR-182 · Metastatic dissemination · SHH pathway · Medulloblastoma

Introduction

Medulloblastoma (MB) remains one of the most challenging diseases in pediatric oncology with considerable mortality and post-treatment morbidity [17]. Recent studies have consistently identified several distinct biological subgroups of MB with distinct genetics, demographics, and clinical outcomes. Subgroup affiliation should prove clinically useful to stratify patients in future MB clinical trials [1, 2, 10, 16, 19, 20, 23]. One unresolved problem remains that metastatic dissemination at diagnosis, which is present in about 30% of MB patients, is associated with a significantly inferior prognosis [3]. Our understanding of the molecular mechanisms contributing to leptomeningeal dissemination is minimal, providing few if any molecular targets to treat or prevent disease progression.

The identification of microRNAs (miRNAs) as mediators of various centrally important cellular processes has been one of the most striking improvements in our understanding of molecular cell function in the last decade. These short, non-coding RNA molecules (21–25 nucleotides) are known to play important roles in tumorigenesis and to display distinct expression signatures within different cancer types [8, 13]. However, the specific roles of miRNAs in the biology of MB, the most frequent malignant brain tumor in childhood remain incompletely understood. The most striking and consistent finding so far has been the involvement of the miR-17–92 cluster as an oncomir in sonic hedgehog-driven MB (SHH-MB) [15, 24].

Corroborating recently reported findings [1], microRNA profiling in a cohort of 32 primary MBs could readily distinguish SHH-MB from non-SHH-MB, which was subsequently validated in an independent tumor cohort studied on a different miRNA expression platform [15]. Subgroup-specific patterns of miRNA expression could be due to different cells of origin [4, 6]. Among the most differentially expressed miRNAs, the retinal miRNAs hsa-miR-182 (miR-182), hsa-miR-183 (miR-183), and hsa-miR-96 (miR-96) [25], demonstrated consistent overexpression in non-SHH-MBs, whereas in SHH-MBs, they were expressed at levels comparable to normal cerebellum. Interestingly, pro-migratory and proliferative effects were recently attributed to miR-182 in breast cancer [14] and melanoma [22], another neuroectodermal tumor, whereas inhibition of proliferation and invasion was reported in lung cancer [26].

In this report, we demonstrate in vitro and in vivo that overexpression of miR-182 in the context of non-SHH-MB drives metastatic dissemination, and that inhibition of miR-182 is a molecular target for the treatment of metastatic MB.

Materials and methods

Clinical materials and microRNA preparation

One hundred and eleven MB samples were included in this study, divided into screening ($n = 32$), validation cohort ($n = 90$), and QRT-PCR-validation cohort ($n = 79$). Detailed clinical information is listed in Table 1 and Supplementary Tables 1/2 and appendix. Molecular subgroups were revealed either by gene expression profiling ($n = 40$) or immunohistochemistry ($n = 71$) as previously described [16, 19, 20]. All clinical samples were collected after informed consent at the Department of Neuropathology, NN Burdenko Neurosurgical Institute, Moscow, Russia.

Snap frozen tissues were homogenized and total RNA was extracted using the miRNeasy kit (Qiagen) following the manufacturer's instruction. RNA quality was assessed using the RNA 6000 Nano kit (Agilent). Samples with a RNA integrity number (RIN) higher than 8.0 were used for further experiments. Our previously published dataset including 90 primary MB samples using a different methodology and platform was used as validation cohort [15].

MicroRNA microarray and bioinformatic analysis

MicroRNA expression profiles of the screening cohort were obtained by the 1,146 Human miRNAs V2, Illumina microRNA DASL array (Illumina). Raw data were normalized by quantile normalization using the Illumina software BeadStudio (ver.3). Normalized data were log2 transformed. Details on the microarray analysis are given in the Supplementary appendix. p values of 0.05 or below were considered significant.

Quantitative real-time PCR

TaqMan MicroRNA Assay (Applied Biosystems) was used to verify the expression levels of candidate miRNAs (hsa-miR-182, ABI assay ID 00597; hsa-miR-183, ABI assay ID 000484) as previously reported [7]. Expression levels of

Table 1 Clinical–pathological characteristics of the patients–screening cohort

Variable	Medulloblastoma subtypes					Fisher's exact test *p*
	SHH 11 (34.4%)	WNT 4 (12.5%)	Group C 3 (9.4%)	Group D 14 (43.8%)	All 32 (100%)	
Age, years						
≤3	3 (27.3%)	0 (0.0%)	1 (33.3%)	0 (0.0%)	4 (12.5%)	0.03
4–17	4 (36.4%)	3 (75.0%)	2 (66.7%)	10 (71.4%)	19 (53.1%)	
≥18	4 (36.4%)	1 (25.0%)	0 (0.0%)	4 (28.6%)	9 (34.4%)	
Gender						
Female	1 (9.1%)	2 (50.0%)	1 (33.3%)	5 (35.7%)	9 (28.1%)	0.25
Male	10 (90.9%)	2 (50.0%)	2 (66.7%)	9 (64.3%)	23 (71.9%)	
Localization						
Hemispheric	8 (72.7%)	1 (25.0%)	0 (0.0%)	1 (7.1%)	10 (31.2%)	< 0.01
Midline	3 (27.3%)	3 (75.0%)	3 (100.0%)	13 (92.9%)	22 (68.8%)	
Histology						
Classic	4 (36.4%)	4 (100.0%)	0 (0.0%)	11 (78.6%)	19 (59.4%)	< 0.01
MBEN/desmoplastic	5 (45.5%)	0 (0.0%)	0 (0.0%)	0 (0.0%)	5 (15.6%)	
LCA	2 (18.2%)	0 (0.0%)	3 (100.0%)	3 (21.4%)	8 (25.0%)	
Metastatic stage						
M0	7 (63.6%)	3 (75.0%)	2 (66.7%)	6 (42.9%)	18 (56.2%)	0.66
M1–3	4 (36.4%)	1 (25.0%)	1 (33.3%)	8 (57.1%)	14 (43.8%)	

MBEN Medulloblastoma with extensive nodularity, *LCA* large cell/anaplastic, *SHH* sonic hedgehog pathway

individual miRNAs were calculated using the 2[-delta delta C(T)] method [12] relative to the average expression level of two housekeeping small RNAs, RNU6B (ABI assay ID 001093) and RNU66 (ABI assay ID 001002), and a pooled normal cerebellum total RNA (24 male/female Caucasian, ages 16–70; Clontech).

Medulloblastoma cell culture

Medulloblastoma cell lines DAOY (Cat#HTB-186, ATCC), D458 Med (kindly provided by Dr. Darell D. Bigner, Duke University, USA) [9], and Med8A (kindly provided by Dr. Michael D. Taylor, University of Toronto, Canada) [11] were selected for functional validation according to their different expression levels of candidate miRNAs (Supplementary Fig. 1a). DAOY and Med8A were cultured in DMEM (Invitrogen) with 10% FBS. D458 Med was cultured in Improved MEM with Zn^{2+} option medium (Invitrogen) with 20% FBS. All MB cell lines were incubated in a 5% CO_2 atmosphere condition.

Stable overexpression and transient knockdown (KD) of miRNA candidates

PCR fragments containing miR-182 (296 bp), or miR-183 (325 bp) were cloned into the pCMX-PL1 vector (pCMX, kindly provided by Dr. Roland Schüle, Medical School Freiburg, Germany) [18]. The primer sequences are provided in Supplementary Table 3. Transfection was carried out with Lipofectamine 2000 (Invitrogen), 25 mM Zeocin (Invitrogen) was applied to the culture medium for stable clone selection; two single colonies with the highest expression level, confirmed by QRT-PCR, were used for further functional studies (Supplementary Fig. 1b). Transient KD of miRNA candidates was carried out by Ambion Anti-miR miRNA Inhibitor (anti-miR-182, AM12369; anti-miR-183, AM12830; ABI). Expression levels of candidate miRNAs were evaluated by QRT-PCR after KD (Supplementary Fig. 1c). Functional assays were carried out 24 h after KD.

Scratch assay

DAOY and Med8A were grown in confluence on a Lab-Tek chambered coverglass (Nunc) in monolayer. After serum starvation for 24 h, a "wound" was made in the middle of the chamber and pictures were taken at the indicated time. Migratory speed was calculated by comparing the final wound width (after 12 h) with the initial width at the beginning of the experiment. The relative migratory speed was determined by preparing a ratio of the migratory speed of the tested cell line compared to the control cell line (pCMX for overexpression, and scrambled negative control for knockdown).

Boyden chamber migration/invasion assay

The migration ability of DAOY and D458Med was measured in transwells with a 8-µm pore polycarbonate membrane insert (Corning). The invasion ability was determined using BD BioCoat Matrigel invasion chambers (BD Biosciences). After serum starvation for 24 h, cells were harvested and resuspended in serum free medium. 1×10^5 cell (DAOY, adhesive cell line) or 5×10^5 cells (D458 Med, half suspension cell line) were seeded in the upper reservoir of the migration and invasion chambers, respectively. Normal culture medium with FBS was added in the lower reservoir as a chemoattractant. After 16 (DAOY) or 24 (D458 Med) hours of incubation, migrated cells were fixed with methanol, stained with haematoxylin, and mounted on a glass slide for cell counting.

3D microchannel migration assay

Poly(dimethylsiloxane) (PDMS) based microchannel chips were kindly provided by Dr. Ralf Kemkemer (Max Planck Institute for Intelligent Systems, Germany). Microfabricated channel structures with the dimensions of $5 \times 11 \times 300$ µm (W × H × L) (Supplementary Fig. 2) were coated with a 50-µg/ml fibronectin solution prior to use. The chip was fixed on a Teflon holder and 2×10^5 cells were seeded on the chip in close proximity to the channels. After cells were attached on the chip, live-cell imaging was started. During the experiments, no chemical gradient or flow inside the channels was applied. Phase-contrast time-lapse pictures of multiple positions were captured for every 10 min with an automated inverted microscope (Zeiss Cell Observer; Carl Zeiss) equipped with a heated and air-humidified chamber. Images were recorded and processed with Zeiss AxioVision and ImageJ software. Cell behaviors were analyzed and categorized as described in Supplementary appendix and reported previously [21].

Medulloblastoma experiments in vivo

5×10^5 DAOY cells with stable transfection of miR-182 or control vector were injected into the left cerebellar hemisphere of CB17/SCID mice (Charles River Laboratories). Details are given in the Supplementary appendix.

Results and discussion

Non-SHH-MB display a distinct miRNA expression pattern that includes overexpression of retinal miRNAs

We determined genome-wide miRNA expression profiles in a screening set of 32 primary MBs (Table 1). Unsupervised hierarchical clustering identified three major groups with SHH-MBs showing the clearest separation from the remaining subgroups (Fig. 1a, Supplementary Fig. 3). Principal component analysis demonstrates the same relationships (Fig. 1b). Based on our overlapping mRNA expression profiling data [19, 20], the molecular subgroups included WNT, SHH, and non-WNT/non-SHH MB variants. Likely due to the low proportion of group C tumors ($n = 3$), group C and D tumors could not be differentiated based on miRNA expression patterns. Fundamental miRNA expression differences between SHH- and non-SHH-MB were determined by significance analysis of microarrays, yielding a robust 26-miRNA signature that could readily separate SHH-MBs from non-SHH-MBs (Supplementary Table 4, Fig. 1c). Validation of the 26-miRNA signature using an independent series of 90 primary MBs (Supplementary Table 1) [15] studied on a different miRNA platform also readily separated SHH from non-SHH tumors (Supplementary Fig. 4). Notably, the retinal miRNA cluster on chromosome 7q32 (miR-182, miR-183, and miR-96) were the most differentially regulated miRNAs within the 26-miRNA signature (Supplementary Table 4). In the validation dataset, the same strong effect was observed for miR-182 and miR-183 (Supplementary Fig. 4). Thus, we focused all subsequent analyses on these two miRNAs that showed consistent results in both independent datasets.

miR-182 and miR-183 are highly overexpressed in non-SHH-MB

The expression levels of miR-182 and miR-183 were subsequently validated by quantitative real-time PCR (QRT-PCR) in the screening cohort ($n = 32$) studied by miRNA profiling, and a non-overlapping QRT-PCR-validation cohort ($n = 79$; Supplementary Table 2). For the screening cohort, QRT-PCR results were closely correlated with the microarray data (Spearman's ρ 0.97, $p < 0.0001$; Supplementary Fig. 5). In the QRT-PCR-validation cohort, we further confirmed that expression levels of both candidate miRNAs were significantly higher in non-SHH-MBs, as compared to SHH-MBs ($p < 0.0001$; Fig. 2a). Likely, due to the heterogeneous prognosis of non-SHH tumors with excellent prognosis of WNT-MBs and intermediate to dismal prognosis of group C and D [16, 19, 20], we observed no prognostic impact of miR-182 and miR-183 expression (data not shown). Importantly, further correlation of the QRT-PCR results with clinical and pathological parameters revealed that MBs located in the cerebellar midline showed a significantly higher expression of both candidate miRNAs ($p < 0.001$), and miR-182 showed a significantly higher expression in metastatic MB ($p = 0.03$; Fig. 2b). These data complement previously published data showing that SHH-MB usually occur

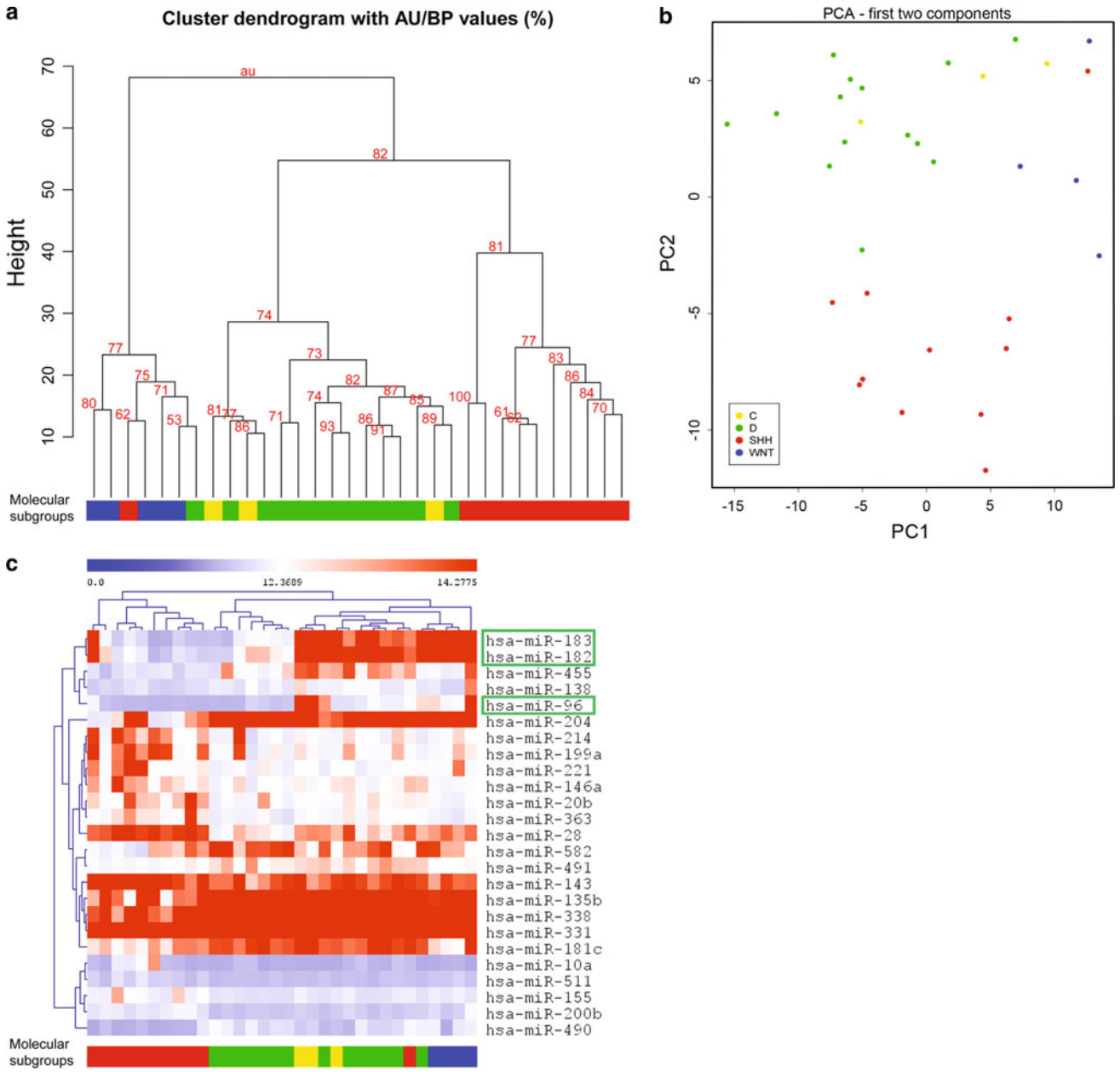

Fig. 1 Genome-wide microRNA expression. MicroRNAs miR-182 and miR-183 are highly up-regulated in non-SHH-MB. Color scheme applies to all figures: SHH (*red*), WNT (*blue*), C (*yellow*), and D (*green*). **a** Unsupervised hierarchical clustering (HCL) of miRNA expression, method: Ward, distance: Euclidean. Predicted molecular subgroup information was obtained from our previous study [19]. **b** Principal component analysis of the screening set showed sonic hedgehog-driven medulloblastomas are distinct from other disease variants regarding their miRNA expression patterns. **c** Supervised HCL of screening set based on the 26-miRNA signature separating SHH-MB from non-SHH-MB, *green boxes* indicate retinal miRNAs, miR-182, miR-183, and miR-96, which were generally overexpressed in non-SHH-MBs. MicroRNA-182 and miR-183 showed distinct expression patterns in the three clusters

laterally in the cerebellar hemisphere [17], and have a lower incidence of metastases [16]. Since miR-182 expression was highly correlated with SHH subtype, the link between miR-182 expression and tumor localization ($p = 0.23$) and metastasis ($p = 0.24$) was not independent of MB subtype. In contrast to an earlier study reporting on the up-regulation of retina miRNAs in WNT-MBs [5], we demonstrate in our large dataset that 'retinal miRNA' overexpression is not limited to WNT-MB, but rather shows high expression levels across all of the non-SHH tumors (Fig. 2a).

Scratch assay reveals pro-migratory effects of miR-182/183 overexpression

Proliferation was not consistently affected by stable overexpression or transient knockdown (KD) of miR-182 and

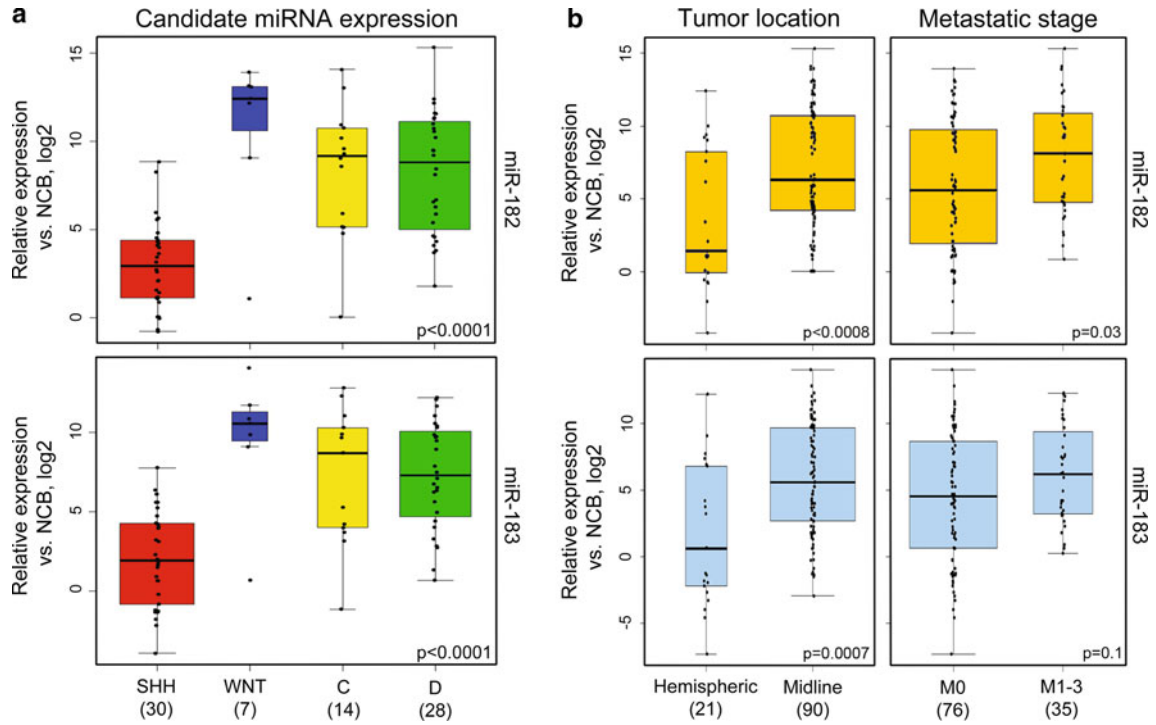

Fig. 2 Quantitative Real-time PCR **a** Validation of miR-182 and miR-183 expression levels by QRT-PCR in test set ($n = 79$). Non-SHH-MBs show significantly higher expression of both candidate miRNAs compared to SHH-MBs. **b** Expression of miR-182 and miR-183 is linked to tumor location and metastatic stage. Both candidates showed higher expression in midline MBs, and miR-182 showed significantly higher expression in metastatic MBs

miR-183 in the MB cell lines DAOY or Med8A (Supplementary Fig. 6). Next, we tested the migratory effects of both candidates. Overexpression of miR-182 in DAOY cells (DAOY-182K1, DAOY-182K2) significantly increased migration speed in scratch assays at least fourfold compared to the empty vector control (DAOY-pCMX) (Dunnett contrasts, $p < 0.001$). In contrast to this, we observed a decreased migratory propensity for DAOY with miR-182 KD (Fig. 3a, b). DAOY with miR-183 overexpression (DAOY-183K1, DAOY-183K2) did not show a clear difference regarding the migratory speed compared to DAOY-pCMX. Knockdown of miR-183, however, also resulted in decreased cell migration (Fig. 3b, c) ($p < 0.001$). A second MB cell line, Med8A, which has a very low baseline expression of miR-182 and miR-183 (Supplementary Fig. 1a) showed a moderate but significant increase in the migratory speed after stable transfection of miR-182 and one miR-183 clone ($p < 0.001$), whereas further KD of these miRNAs did not show any significant changes in the migratory speed of Med8A (Fig. 3b, c).

3D microchannel assay confirms the pro-migratory effect of miR-182

A micro-fabricated device with channel structures mimicking a 3D in vivo environment was used to monitor cell migration by time-lapse imaging. This technique, in comparison to the classic Boyden chamber assay, allows the user to follow single cell migration though accurately defined structures in real-time. The interaction between cells and the channels was categorized into three activities: penetration, invasion, and permeation [21]. Time-lapse pictures in Fig. 3d (taken from Video 1) show an example of a DAOY cell permeating a 5-µm wide channel (all three different cell behaviors are demonstrated in Video 1–4). The invasiveness of cells is defined as the percentage of invasive and permeative cells of all cells that were trying to enter the channels. Stable overexpression of miR-182 increased the average invasiveness 2.6-fold (DAOY-182K1) and 2.9-fold (DAOY-182K2) compared to DAOY-pCMX, respectively (Dunnett contrasts, $p < 0.001$). Inversely, DAOY with transient KD of miR-182 showed a significantly reduced invasiveness of 0.6-fold as compared to negative controls (Dunnett contrasts, $p = 0.03$, Fig. 3e). In line with these observations, upon miR-182 overexpression in Med8A cells, we observed a trend towards an increased migratory and invasive phenotype (Fig. 3f; Video 5, Video 6). Notably, Med8A-pCMX cells showed no migratory behavior and were not capable of invading the 5-µm channels.

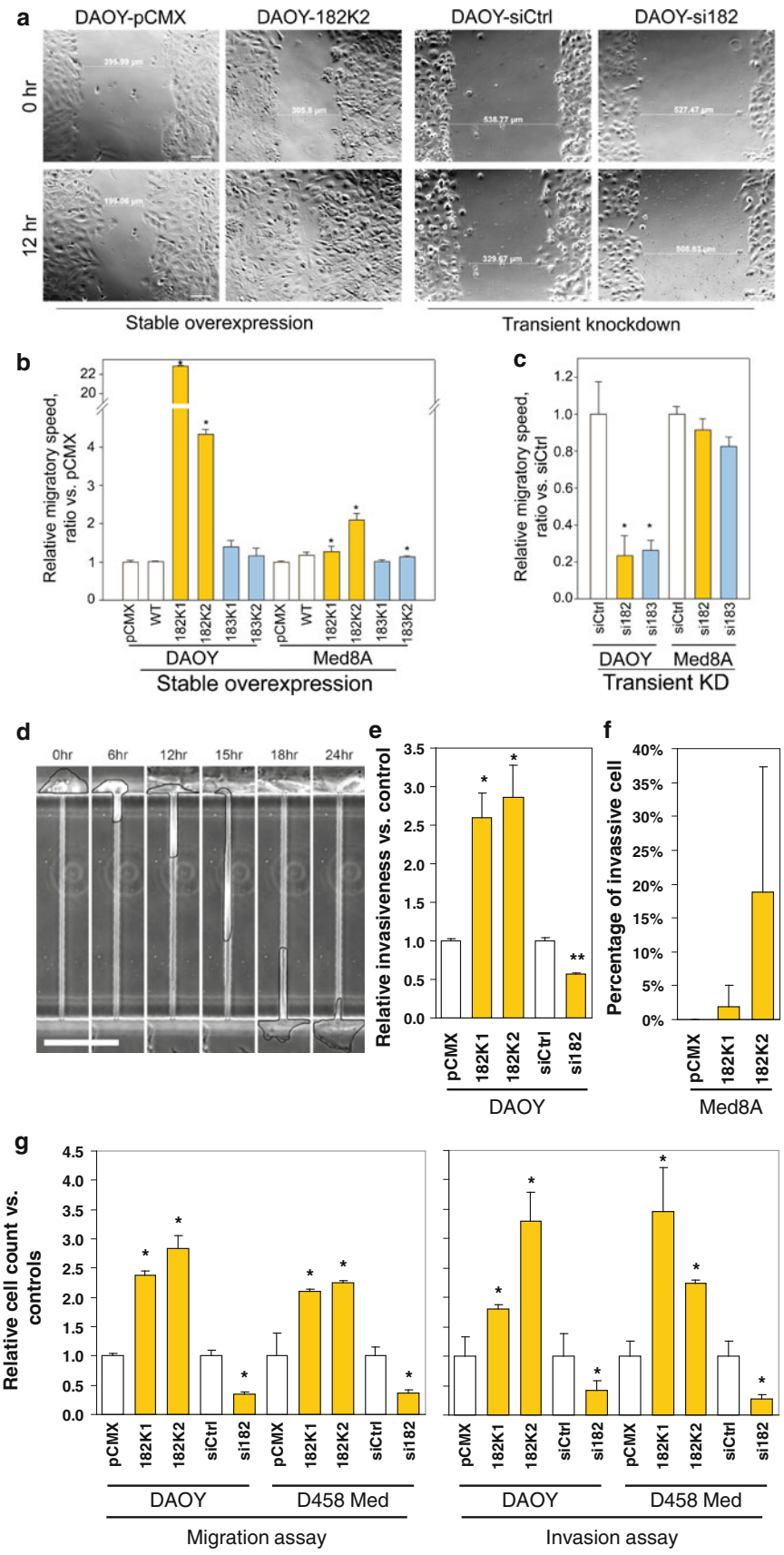

Fig. 3 In vitro migration studies. **a** Representative images of scratch assay after stable overexpression and transient knockdown (KD) of miR-182 in DAOY. *Scale bar* 100 μm. **b** Overexpression of miR-182 showed a dramatic impact on the migration speed of both DAOY and Med8A cell (Dunnett contrasts, $*p < 0.001$). **c** Transient KD of miR-182 and miR-183 showed a significant effect on the migration speed of DAOY only (Dunnett contrasts, $*p < 0.001$). **d** Images from time-lapse video, a DAOY cell permeating a $5 \times 11 \times 300$-μm channel. The outline of the DAOY cell was manually marked with *black lines* for better visualization. *Scale bar* 100 μm. **e** 3D Micro-channel assay showed that the relative invasiveness was doubled in both single DAOY colonies with miR-182 overexpression, and was decreased by ~50% after siRNA treatment compared to empty vector transfected control (pCMX) and scramble negative siRNA treatment control (siCtrl) (Dunnett contrasts, $*p < 0.001$; $**p = 0.03$). **f** No invasive cells were observed in Med8A with empty vector (pCMX), but observed in both single colonies with miR-182 overexpression (Med8A-182K1: $p = 0.37$, Med8A-182K2: $p = 0.12$). Basal migration was 0% for Med8A-pCMX, such that it was not possible to provide a fold change here rather than an absolute frequency. All *error bars* indicate the mean ± SD of three independent experiments. **g** Boyden chamber assays confirmed that miR-182 expression is significantly associated with the pro-migratory phenotype of DAOY and D458 Med cells

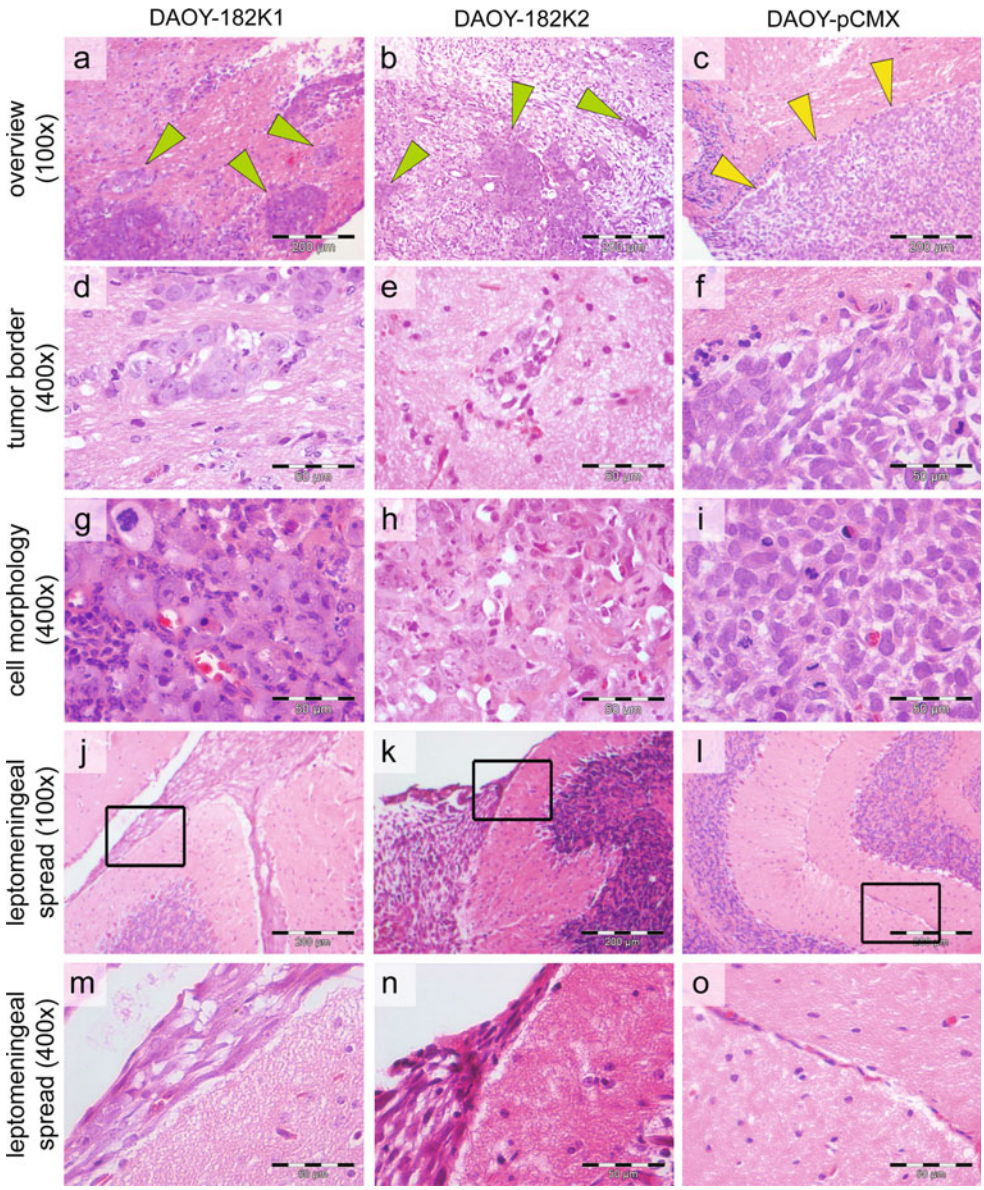

Fig. 4 Haematoxylin & eosin staining of DAOY xenograft sections. **a**, **b** Both DAOY-182K1 and DAOY-182K2 invaded into the adjacent normal brain, forming small colonies, indicated by *green arrowheads*. **c** DAOY-pCMX formed xenografts with a clear boundary towards normal brain, indicated by *yellow arrowheads*. **d**, **e** Magnified view of the infiltrating colonies of DAOY-182K1 and DAOY-182K2 into the normal brain. **f** Magnified view of the boundary between normal brain and a DAOY-pCMX xenograft. **g–i** Both DAOY-182K1 and DAOY-182K2 showed larger cellular size than DAOY-pCMX morphologically resembling large cell medulloblastoma, which is associated with a highly malignant and invasive clinical phenotype. **j–o** A higher incidence of leptomeningeal spread was seen in tumors overexpressing miR182 compared to controls (*black boxes* position of the ×400 image in the ×100 image)

Boyden chamber assay confirms the pro-migratory effect of miR-182 is not a unique phenotype of DAOY cells

In line with the scratch assay and 3D microchannel assay data, DAOY cells with miR-182 overexpression showed an at least twofold increment of migration compared to empty vector in the migration and invasion assays. A significant reduction of cell migration was noted upon KD of miR-182 in DAOY cells. To confirm these observations in another MB cell line, D458 Med with very high expression level of miR-182 (Supplementary Fig. 1a) was also subjected to Boyden chamber assays upon stable overexpression and KD of miR-182. Both migration and invasion assay showed a significant increase of migrated cells upon miR-182 overexpression in D458Med cells (182K1, 182K2 in Fig. 3g). Conversely, transient KD of miR-182 resulted in decreased migration (Fig. 3g). Taken together, these findings confirmed that miR-182 has an important role in the pro-migratory phenotype of MB cells in vitro.

Overexpression of miR-182 induced invasive MB growth in vivo

To further assess the pro-migratory properties of miR-182 in vivo, we performed orthotopic xenograft experiments of vector control DAOY cells as compared to those overexpressing miR-182. MRI revealed mean tumor formation at 4.6 months (range 3–7) after implantation. Haematoxylin & eosin staining of xenograft sections demonstrated tumor formation by all clones irrespective of the transfected construct (tumor incidence of xenografts in injected

mice: pCMX 4/5 mice, 182K1 4/6 mice, 182K2 2/2 mice). All of the xenografts from DAOY-182K1 and DAOY-182K2 extensively infiltrated the surrounding normal tissue, giving rise to countless small colonies widely distributed throughout the cerebellum (green arrowheads in Fig. 4a, b, d, e), whereas all of the tumor formed by the control clone DAOY-pCMX displayed a clear boundary (Fig. 4c, f). Notably, all of the xenografts derived from DAOY-182K1, and DAOY-182K2 showed a similar morphology, with larger cells reminiscent of large cell/anaplastic MB, in contrast to the morphology of the xenografts derived from the control clones (Fig. 4g–i). Furthermore, leptomeningeal spread was seen only in miR182 overexpressing tumors (K1: 3/4 tumors, 1/4 was dead from tumor before a histological evaluation could be performed; K2: 2/2 tumors) compared to controls, which showed no leptomeningeal spread (pCMX 0/4 tumors) (Fig. 4j–o). Only the local leptomeninges but not the CSF or spinal cords were studied, hence it remains to be elucidated if distant spread in the form of circulating cells in the CSF is also present in the mice with miR-182 overexpressing xenografts. Overexpression of miR-182 did not affect the latency of the xenograft formation, in keeping with our in vitro results on cell proliferation (Supplementary Fig. 6).

In conclusion, our study provides both in vitro and in vivo evidence for an important role of miR-182 in leptomeningeal spread of non-SHH-MB. By elucidating the biology of metastatic MB, novel targeted treatment approaches might be developed for these tumors with particularly dismal prognosis.

Acknowledgments We gratefully thank the patients and families for participating in this research. Jennifer Diemer and Anna Schöttler are acknowledged for excellent technical assistance. Support by the DKFZ Light Microscopy Facility is gratefully acknowledged. This study was supported by a grant from the Deutsche Kinderkrebsstiftung and from the "Tumorzentrum Heidelberg" to S.M.P.; a "Young Investigator Fellowship" of the Medical Faculty of Heidelberg and financial support by the Eliteprogramme for Postdocs (Baden-Württemberg Stiftung) to M.R.

Conflict of interest The authors declare no conflicts of interest.

References

1. Cho Y-J, Tsherniak A, Tamayo P, Santagata S, Ligon A, Greulich H, Berhoukim R, Amani V, Goumnerova L, Eberhart CG, Lau CC, Olson JM, Gilbertson RJ, Gajjar A, Delattre O, Kool M, Ligon K, Meyerson M, Mesirov JP, Pomeroy SL (2011) Integrative genomic analysis of medulloblastoma identifies a molecular subgroup that drives poor clinical outcome. J Clin Oncol 29(11):1424–1430
2. Ellison DW, Kocak M, Dalton J, Megahed H, Lusher ME, Ryan SL, Zhao W, Nicholson SL, Taylor RE, Bailey S, Clifford SC (2011) Definition of disease-risk stratification groups in childhood medulloblastoma using combined clinical, pathologic, and molecular variables. J Clin Oncol 29(11):1400–1407. doi:10.1200/JCO.2010.30.2810
3. Fouladi M, Gajjar A, Boyett JM, Walter AW, Thompson SJ, Merchant TE, Jenkins JJ, Langston JW, Liu A, Kun LE, Heideman RL (1999) Comparison of CSF cytology and spinal magnetic resonance imaging in the detection of leptomeningeal disease in pediatric medulloblastoma or primitive neuroectodermal tumor. J Clin Oncol 17(10):3234–3237
4. Gibson P, Tong Y, Robinson G, Thompson MC, Currle DS, Eden C, Kranenburg TA, Hogg T, Poppleton H, Martin J, Finkelstein D, Pounds S, Weiss A, Patay Z, Scoggins M, Ogg R, Pei Y, Yang ZJ, Brun S, Lee Y, Zindy F, Lindsey JC, Taketo MM, Boop FA, Sanford RA, Gajjar A, Clifford SC, Roussel MF, McKinnon PJ, Gutmann DH, Ellison DW, Wechsler-Reya R, Gilbertson RJ (2010) Subtypes of medulloblastoma have distinct developmental origins. Nature 468(7327):1095–1099. doi:10.1038/nature09587
5. Gokhale A, Kunder R, Goel A, Sarin R, Moiyadi A, Shenoy A, Mamidipally C, Noronha S, Kannan S, Shirsat NV (2010) Distinctive microRNA signature of medulloblastomas associated with the WNT signaling pathway. J Cancer Res Ther 6(4):521–529. doi:10.4103/0973-1482.77072
6. Goodrich LV, Milenkovic L, Higgins KM, Scott MP (1997) Altered neural cell fates and medulloblastoma in mouse patched mutants. Science 277(5329):1109–1113
7. Gronych J, Korshunov A, Bageritz J, Milde T, Jugold M, Hambardzumyan D, Remke M, Hartmann C, Witt H, Jones DT, Witt O, Heiland S, Bendszus M, Holland EC, Pfister S, Lichter P (2011) An activated mutant BRAF kinase domain is sufficient to induce pilocytic astrocytoma in mice. J Clin Invest 121(4):1344–1348. doi:10.1172/JCI44656
8. He L, Thomson JM, Hemann MT, Hernando-Monge E, Mu D, Goodson S, Powers S, Cordon-Cardo C, Lowe SW, Hannon GJ, Hammond SM (2005) A microRNA polycistron as a potential human oncogene. Nature 435(7043):828–833. doi:10.1038/nature03552
9. He XM, Wikstrand CJ, Friedman HS, Bigner SH, Pleasure S, Trojanowski JQ, Bigner DD (1991) Differentiation characteristics of newly established medulloblastoma cell lines (D384 Med, D425 Med, and D458 Med) and their transplantable xenografts. Lab Invest 64(6):833–843
10. Kool M, Koster J, Bunt J, Hasselt NE, Lakeman A, van Sluis P, Troost D, Meeteren NS, Caron HN, Cloos J, Mrsic A, Ylstra B, Grajkowska W, Hartmann W, Pietsch T, Ellison D, Clifford SC, Versteeg R (2008) Integrated genomics identifies five medulloblastoma subtypes with distinct genetic profiles, pathway signatures and clinicopathological features. PLoS One 3(8):e3088. doi:10.1371/journal.pone.0003088
11. Langdon JA, Lamont JM, Scott DK, Dyer S, Prebble E, Bown N, Grundy RG, Ellison DW, Clifford SC (2006) Combined genome-wide allelotyping and copy number analysis identify frequent genetic losses without copy number reduction in medulloblastoma. Genes Chromosom Cancer 45(1):47–60. doi:10.1002/gcc.20262
12. Livak KJ, Schmittgen TD (2001) Analysis of relative gene expression data using real-time quantitative PCR and the 2(-Delta Delta C(T)) method. Methods 25(4):402–408. doi:10.1006/meth.2001.1262
13. Lu J, Getz G, Miska EA, Alvarez-Saavedra E, Lamb J, Peck D, Sweet-Cordero A, Ebert BL, Mak RH, Ferrando AA, Downing JR, Jacks T, Horvitz HR, Golub TR (2005) MicroRNA expression profiles classify human cancers. Nature 435(7043):834–838. doi:10.1038/nature03702
14. Moskwa P, Buffa FM, Pan Y, Panchakshari R, Gottipati P, Muschel RJ, Beech J, Kulshrestha R, Abdelmohsen K, Weinstock

DM, Gorospe M, Harris AL, Helleday T, Chowdhury D (2011) miR-182-mediated downregulation of BRCA1 impacts DNA repair and sensitivity to PARP inhibitors. Mol Cell 41(2):210–220. doi:10.1016/j.molcel.2010.12.005

15. Northcott PA, Fernandez LA, Hagan JP, Ellison DW, Grajkowska W, Gillespie Y, Grundy R, Van Meter T, Rutka JT, Croce CM, Kenney AM, Taylor MD (2009) The miR-17/92 polycistron is up-regulated in sonic hedgehog-driven medulloblastomas and induced by N-myc in sonic hedgehog-treated cerebellar neural precursors. Cancer Res 69(8):3249–3255. doi:10.1158/0008-5472.CAN-08-4710
16. Northcott PA, Korshunov A, Witt H, Hielscher T, Eberhart CG, Mack S, Bouffet E, Clifford SC, Hawkins CE, French P, Rutka JT, Pfister S, Taylor MD (2011) Medulloblastoma comprises four distinct molecular variants. J Clin Oncol 29(11):1408–1414. doi:10.1200/jco.2009.27.4324
17. Polkinghorn WR, Tarbell NJ (2007) Medulloblastoma: tumorigenesis, current clinical paradigm, and efforts to improve risk stratification. Nat Clin Pract Oncol 4(5):295–304. doi:10.1038/ncponc0794
18. Pscherer A, Schliwka J, Wildenberger K, Mincheva A, Schwaenen C, Dohner H, Stilgenbauer S, Lichter P (2006) Antagonizing inactivated tumor suppressor genes and activated oncogenes by a versatile transgenesis system: application in mantle cell lymphoma. FASEB J 20(8):1188–1190. doi:10.1096/fj.05-4854fje
19. Remke M, Hielscher T, Korshunov A, Northcott PA, Bender S, Kool M, Westermann F, Benner A, Cin H, Ryzhova M, Sturm D, Witt H, Haag D, Toedt G, Wittmann A, Schöttler A, von Bueren AO, von Deimling A, Rutkowski S, Scheurlen W, Kulozik AE, Taylor MD, Lichter P, Pfister SM (2011) FSTL5 is a marker of poor prognosis in non-WNT/non-SHH medulloblastoma. J Clin Oncol 29(29):3852–3861
20. Remke M, Hielscher T, Northcott PA, Witt H, Ryzhova M, Wittmann A, Benner A, von Deimling A, Scheurlen W, Perry A, Croul S, Kulozik AE, Lichter P, Taylor MD, Pfister SM, Korshunov A (2011) Adult medulloblastoma comprises three major molecular variants. J Clin Oncol 29(19):2717–2723. doi:10.1200/JCO.2011.34.9373
21. Rolli CG, Seufferlein T, Kemkemer R, Spatz JP (2010) Impact of tumor cell cytoskeleton organization on invasiveness and migration: a microchannel-based approach. PLoS One 5(1):8726. doi:10.1371/journal.pone.0008726
22. Segura MF, Hanniford D, Menendez S, Reavie L, Zou X, Alvarez-Diaz S, Zakrzewski J, Blochin E, Rose A, Bogunovic D, Polsky D, Wei J, Lee P, Belitskaya-Levy I, Bhardwaj N, Osman I, Hernando E (2009) Aberrant miR-182 expression promotes melanoma metastasis by repressing FOXO3 and microphthalmia-associated transcription factor. Proc Natl Acad Sci USA 106(6):1814–1819. doi:10.1073/pnas.0808263106
23. Thompson MC, Fuller C, Hogg TL, Dalton J, Finkelstein D, Lau CC, Chintagumpala M, Adesina A, Ashley DM, Kellie SJ, Taylor MD, Curran T, Gajjar A, Gilbertson RJ (2006) Genomics identifies medulloblastoma subgroups that are enriched for specific genetic alterations. J Clin Oncol 24(12):1924–1931. doi:10.1200/JCO.2005.04.4974
24. Uziel T, Karginov FV, Xie S, Parker JS, Wang YD, Gajjar A, He L, Ellison D, Gilbertson RJ, Hannon G, Roussel MF (2009) The miR-17 92 cluster collaborates with the Sonic Hedgehog pathway in medulloblastoma. Proc Natl Acad Sci USA 106(8):2812–2817. doi:10.1073/pnas.0809579106
25. Xu S, Witmer PD, Lumayag S, Kovacs B, Valle D (2007) MicroRNA (miRNA) transcriptome of mouse retina and identification of a sensory organ-specific miRNA cluster. J Biol Chem 282(34):25053–25066. doi:10.1074/jbc.M700501200
26. Zhang L, Liu T, Huang Y, Liu J (2011) microRNA-182 inhibits the proliferation and invasion of human lung adenocarcinoma cells through its effect on human cortical actin-associated protein. Int J Mol Med 28(3):381–388. doi:10.3892/ijmm.2011.679